TECHNIQUE ARTICLE
Cytoskeleton, November 2013 70:706–717 (doi: 10.1002/cm.21136)
Published 2013 Wiley-Periodicals, Inc.†

The Design of MACs (Minimal Actin Cortices)

Sven K. Vogel,* Fabian Heinemann, Grzegorz Chwastek, and Petra Schwille

Department of Cellular and Molecular Biophysics, Max Planck Institute of Biochemistry, Martinsried, Germany

Received 12 July 2013; Revised 14 August 2013; Accepted 12 August 2013
Monitoring Editor: Laura Machesky

The actin cell cortex in eukaryotic cells is a key player in controlling and maintaining the shape of cells, and in driving major shape changes such as in cytokinesis. It is thereby constantly being remodeled. Cell shape changes require forces acting on membranes that are generated by the interplay of membrane coupled actin filaments and assemblies of myosin motors. Little is known about how their interaction regulates actin cell cortex remodeling and cell shape changes. Because of the vital importance of actin, myosin motors and the cell membrane, selective in vivo experiments and manipulations are often difficult to perform or not feasible. Thus, the intelligent design of minimal in vitro systems for actin-myosin-membrane interactions could pave a way for investigating actin cell cortex mechanics in a detailed and quantitative manner. Here, we present and discuss the design of several bottom-up in vitro systems accomplishing the coupling of actin filaments to artificial membranes, where key parameters such as actin densities and membrane properties can be varied in a controlled manner. Insights gained from these in vitro systems may help to uncover fundamental principles of how exactly actin-myosin-membrane interactions govern actin cortex remodeling and membrane properties for cell shape changes.

Key Words: actin; myosin; membrane; actin cortex; actomyosin

Introduction

The use of minimal systems in the field of cytoskeletal and motor protein research is and was a story of great discoveries and successes. Reconstituted minimal systems gave deep mechanistic insights into the properties of cytoskeletal and motor proteins, which led to uncovering general underlying principles and helped to understand their functions inside living cells [Mitchison and Kirschner, 1984; Spudich et al., 1985; Vale et al., 1985]. In most of these studies, cytoskeletal proteins were investigated as isolated systems combined with motor proteins or other accessory proteins [Spudich et al., 1985; Loisel et al., 1999]. Nevertheless, fundamental processes such as cell division, cell locomotion, and any cell shape changes strongly rely on direct interaction between the cytoskeleton, in particular, the actin cytoskeleton, and the cell membrane. The region where actin-membrane interactions drive cell shape changes is referred to as the actin cell cortex, which comprises a thin layer of an actin meshwork beneath the cell membrane. Here, at the cytoskeleton-membrane interface, actin filaments together with assemblies of motor proteins (nonmuscle myosin II) and accessory proteins act together to quickly reorganize the actin cytoskeleton and to exert forces on the membrane, leading to cell shape changes [Heisenberg and Bellaiche, 2013]. The formation and contraction of the actomyosin ring, which is essential to physically split eukaryotic cells into two is probably one of the most prominent examples of such dramatic actin cortex remodeling and force generation acting on the cell membrane. Many proteins have been identified that are part of the actomyosin ring machinery [Glotzer, 2005; Wu et al., 2006]. However, how the ring is formed, how it constricts, and what forces act on the membrane remained unknown [Balasubramanian et al., 2012].

Many in vivo studies have identified the important roles of the actin cytoskeleton and accessory proteins, including molecular motors, in changing the shape of the cell [Wessells et al., 1971; Cramer and Mitchison, 1995]. However, a detailed mechanistic insight in how actin-membrane interactions govern cell shape changes is still missing. Hence, it seems appropriate to investigate the communication between the cytoskeleton and the membrane that lead to cell shape changes in a detailed and quantitative manner. Due to the vital roles of the actin cytoskeleton and the cell membrane, systemic genetic or biochemical perturbations

*Address correspondence to: Sven K. Vogel; Department of Cellular and Molecular Biophysics, Max Planck Institute of Biochemistry, Am Klopferspitz 18, D-82152 Martinsried, Germany.
E-mail: svogel@biochem.mpg.de
Published online 4 October 2013 in Wiley Online Library (wileyonlinelibrary.com).

of living cells may very often lead to severe dysfunctions of cellular processes, and eventually to cell death, largely obstructing mechanistic studies from scratch. Local biochemical or mechanical manipulations are, on the other hand, often difficult to perform and may need the use of sophisticated equipment [Ikai and Afrin, 2003]. Apart from the difficulties in manipulating living cells, one will also face the vast complexity and redundancy of processes at the cytoskeleton-membrane interface. Choosing a reductionist approach by using bottom-up in vitro systems may be the proper approach to uncover general principles of how the interaction between the cytoskeleton and the membrane governs cell shape changes. As in the field of membrane research, the use of minimal model systems proved to be very successful, it may be about time to combine both, cytoskeletal and membrane in vitro systems, in order to understand their interplay. The development of such functional minimal systems for cytoskeleton-membrane interplay has recently begun but is still in its infancy [Vogel and Schwille, 2012]. In this article, we will present various minimal in vitro systems that mimic an actin cell cortex where parameters such as actin density and membrane properties can be easily varied in a controlled manner. Supported and freestanding membranes coupled to actin filaments form the basis of these reconstituted systems, and we will discuss recent results and their potential value for future prospects.

Results

Strategies of Anchoring Actin to the Membrane

As outlined above, cytoskeleton and membrane in vitro systems have been investigated mainly as isolated parts. The combination of these individual units may help to potentially uncover general principles underlying membrane shape changes governed by the interplay between the actin cytoskeleton and membranes. Obviously, the most crucial preparative step is to accomplish a reliable and controllable anchoring strategy to attach the actin filaments in the way that mechanical perturbations of the actin network can be actually transmitted to the membrane. In the past, several different strategies have been proposed, which will be briefly mentioned in the following (see also Vogel and Schwille [2012]). First attempts to anchor actin filaments to artificial membranes were mainly mediated by bivalent magnesium ions (Mg^{2+}) or positively charged lipids, which bind the negatively charged actin filaments [Hackl et al., 1998; Deme et al., 2000; Limozin et al., 2003, 2005]. In order to mimic cell like conditions cell-derived or recombinant proteins that anchor actin filaments to the lipid bilayers such as ezrin or ponticulin were also used [Tanaka and Sackmann, 2005; Johnson et al., 2006; Barfoot et al., 2008; Janke et al., 2008; Bosk et al., 2011]. Other groups made use of L-α-phosphatidylinositol-4,5-bisphosphate (PiP_2) which binds to N-WASP that in combination with the Arp2/3 complex initiates dendritic actin network growth [Blanchoin et al., 2000] thereby nucleating and anchoring actin to the membrane [Liu and Fletcher, 2006; Pontani et al., 2009; Lee et al., 2010]. Another example to mimic physiological conditions was provided by Merkle et al. who purified lipid extracts and the actin anchoring spectrin/ankyrin protein complex from porcine brain extracts [Merkle et al., 2008]. However, the recent use of biotinylated lipids and streptaividin as a possible actin anchoring system [Tsai et al., 2011; Vogel et al., 2013] may represent a good compromise between the various choices of physiological and artificial anchoring systems, as both components are relatively easy to handle, display a very high reproducibility in various in vitro assays and are commercially available thereby avoiding laborious or difficult protein and lipid purifications.

Minimal Actin Cortex (MAC) on Supported Lipid Bilayers

In order to study the actin-membrane interface with highest stability (and thus, reproducibility) of the model system, supported membranes are certainly the assay of choice. At the same time, we aim at building an easily accessible system, supportive of additional manipulations, for example, adding or removing components, and high-resolution light microscopic imaging. A straightforward way to achieve this was to form a lipid bilayer on a transparent solid support such as glass (or Mica), an established method in the field of membrane research [Tamm and McConnell, 1985]. The glass, which may be a microscope slide, is carefully cleaned and plasma treated before a cut synthetic tube (e.g., Eppendorf tube) is glued on top of the glass (Fig. 1A). To form the lipid bilayer, SUVs are then added to the system. SUVs frequently burst when coming in contact with the glass surface, and thus start to assemble into a membrane (step 1 in Fig. 1A). Remaining vesicles can be removed by repetitive washing with a buffer solution. In order to accomplish the anchoring, in this assay, the lipid bilayer contains functionalized biotinylated lipids that bind to neutravidin, a derivate of streptavidin (step 2 in Fig. 1A).

After the remaining neutravidin is washed away, biotinylated actin filaments (phalloidin stabilized or nonstabilized) are added to the system that bind to the biotinylated lipids via neutravidin and form a quasi two-dimensional (2D) actin layer on the membrane (step 3 in Figs. 1A and 1B). The advantage of using the described artificial linker system over the more natural linker systems described beforehand is the tight control over parameters such as the actin density (Fig. 1B). An increase of the amount of biotinylated lipids present in the lipid bilayer leads to an increase in the actin density (Fig. 1B). Saturation of neutravidin and eventual actin binding is reached at approximately 1–2 mol % of the biotinylated lipid (Fig. 1B right image). We noticed that

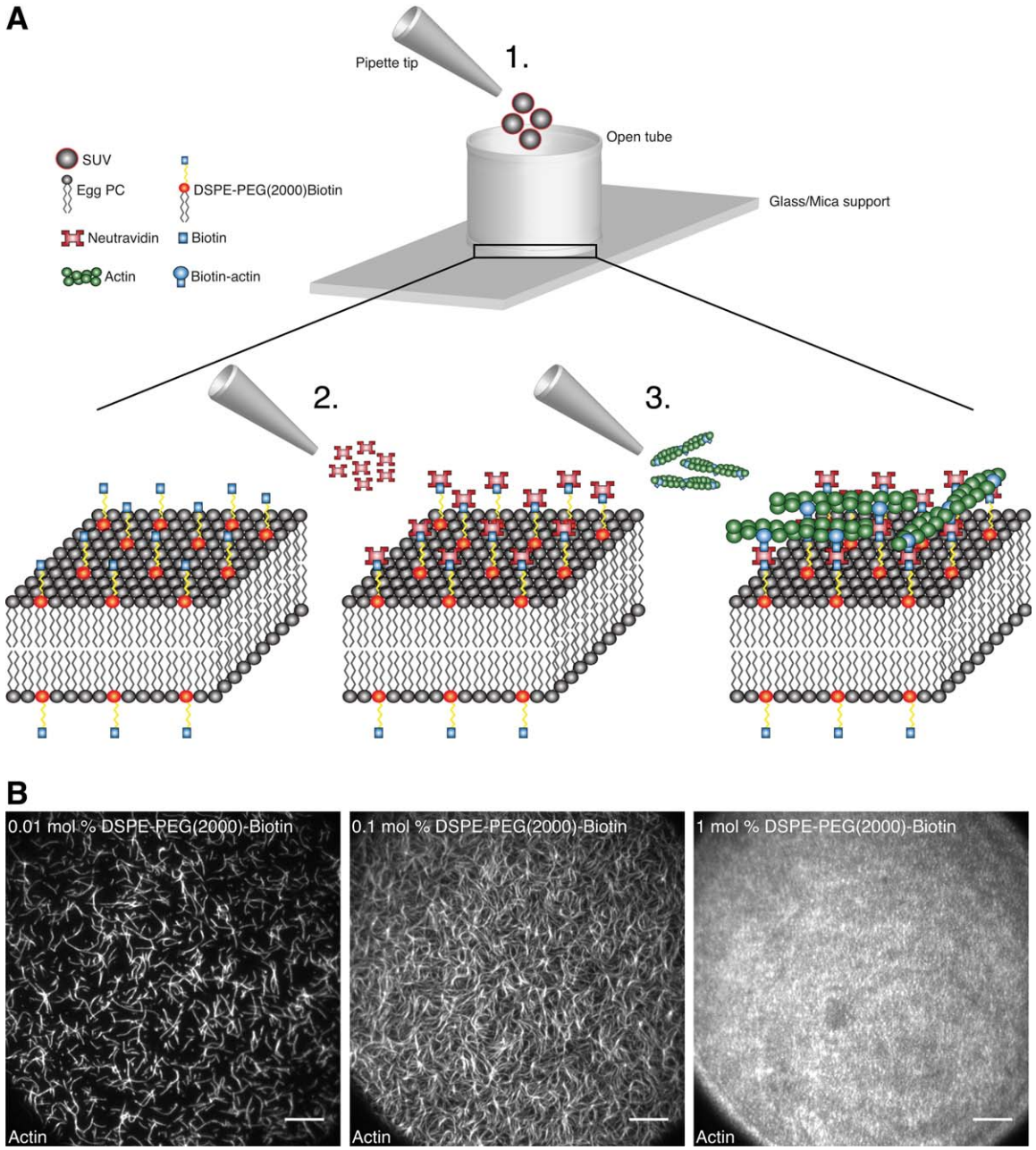

Fig. 1. Steps of MAC composition and actin layers of different densities. (**A**) Schematic representation and steps of the MAC formation. The addition of SUVs (step 1) to the support leads to the formation of a supported lipid bilayer (Egg PC) containing biotinylated lipids (DSPE-PEG(2000)-Biotin). Addition of neutravidin (step 2) and biotinylated actin filaments (step 3) result in their coupling to the lipid bilayer. (**B**) TIRFM images of MACs containing Alexa-488-phalloidin labeled actin filaments. The actin filament density increases from the left to the right image and refers to an increase in the amount of DSPE-PEG(2000)-Biotin (0.01 mol %, 0.1 mol %, and 1 mol %) in the membrane. Scale bars, 10 μm.

only the use of PEGylated biotinylated lipids (DSPE-PEG (2000) Biotin) ensured accurate control over the actin density. Other biotinylated lipids such as Biotinyl PE and Biotinyl Cap did bind actin filaments to some extent, however, neither high actin densities nor an accurate control over the actin density were achieved (data not shown). Since binding of neutravidin (and eventually actin filaments) to Biotinyl Cap lipids is slightly higher than using Biotinyl PE (Biotinyl Cap lipids have a longer spacer between the headgroup and the biotin than Biotinyl PE lipids), we assume that a spacer with a certain length is necessary for proper neutravidin binding to the biotinylated lipid. A relatively long spacer between biotin and the head group of the lipid as in the case of PEGylated lipids may provide more flexibility, thereby decreasing steric hindrance and increasing neutravidin binding. In addition, the number of the anchor points along an actin filament can be also easily varied by the amount of biotinylated actin monomers present in the

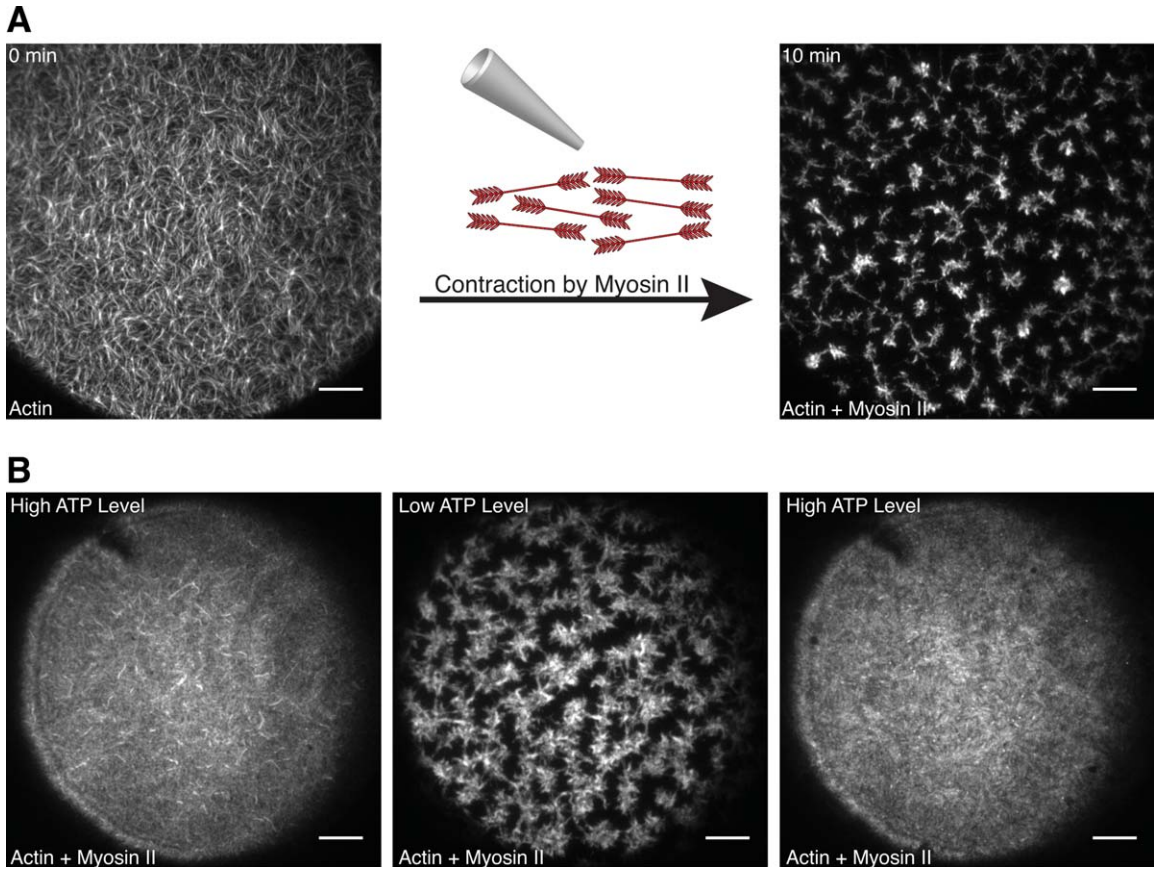

Fig. 2. ATP dependent MAC contraction by myosin motors. (**A**) TIRFM images of a MAC with medium actin density containing Alexa-488-phalloidin labeled actin filaments before (left image) and after (right image) the addition of myofilaments. The myofilament (0.3 μM) driven contraction of the system led to the formation of actomyosin clusters (right image). The ATP concentration (1 μM) here was kept constant. (**B**) TIRFM image series of a MAC with high actin density containing dynamic Alexa-488-labeled actin filaments in the presence of myofilaments. At high ATP concentration (4 mM, left image), the system did not contract. After ATP depletion by the myofilaments at low ATP concentration, the system contracted to form actomyosin clusters (middle image). After readjustment to a high ATP concentration (>4 mM), the system relaxed and an actin layer of high density was formed again (right image). Scale bars, 10 μm.

filaments. As it represents an open system, additional components can be added or removed later on.

ATP Dependent Actin Pattern Formation Induced by Myosin Motors

In most eukaryotic cells, there are at least two general processes required for driving any kind of cell shape changes: One is the quick remodeling of the actin cytoskeleton and the second is force generation exerted on membranes. Both is often executed with the aid of assemblies of the force producing motor protein myosin (myofilaments), that have been proposed to be involved in actin turnover, which is pivotal for fast remodeling of the cytoskeleton during cell shape changes and cytokinesis [Guha et al., 2005; Murthy and Wadsworth, 2005]. Although the main players are known, mechanistic understanding on how force production of the myosin motor assemblies lead to contractility and how they contribute to actin turnover is not known. Thus, our in vitro system may pave the way to uncover general principles of how myosin motors contribute to contractility and turnover in membrane-bound actin meshworks.

As a first step, we found that in our system the addition of synthetic assemblies of myosin II motors, which we will refer from now on as myofilaments, led to the overall contraction of the actin meshwork, dynamic rearrangements of actin filaments during the contraction within the actin mesh, and eventually to the formation of actomyosin clusters within minutes (Fig. 2A); see also Vogel et al. [2013]. We further found that myofilaments acting on single actin filaments fragment and compact these single filaments [Vogel et al., 2013]. In similar assays, also actin filament severing by myofilaments has been observed [Murrell and Gardel, 2012]. We propose that the observed severing of the actin filaments by myofilaments in vitro could be a potential mechanism for a myosin-induced actin turnover in cells.

The process of actin pattern formation and the fragmentation and compaction of single actin filaments in our in vitro system is an ATP dependent process and occurred

only at low ATP concentrations in the range between 0.1 and 1 μM in ATP regenerated systems (see also Vogel et al. [2013]). Starting with a high ATP concentration where ATP is not enzymatically regenerated, and in the presence of myofilaments, the consumption of ATP by the myofilaments led to a decrease in ATP concentration and eventually to actin pattern formation at low ATP levels within minutes (Fig. 2B). Readjusting the ATP concentration to high levels restored the contracted actomyosin pattern to a homogeneously distributed actin layer similar to the starting situation at high ATP concentration (Fig. 2B). Therefore, the ATP concentration can be used as a switch between contractile and relaxed states. We explain the relaxation of the system at high ATP levels as a consequence of the decrease of the duty ratio of the myofilaments [Soares e Silva et al., 2011; Vogel et al., 2013]. Herewith, we try to mimic the fast remodeling and switching behavior present in cells during different cell cycle stages. A similar switching behavior between different states of actin organization depending on the level of ATP has been also observed in other "nonmembrane" in vitro systems [Backouche et al., 2006; Smith et al., 2007; Kohler et al., 2011; Soares e Silva et al., 2011; Gordon et al., 2012]. Although unlikely, it is tempting to speculate that these processes may be also controlled by potential spatiotemporal variations of the ATP concentrations present in cells [Imamura et al., 2009].

MACs on Freestanding Lipid Bilayers

A feature of supported membranes is the frictional coupling between the membrane and the support, which slows down the lateral diffusion of the lipids in the membrane. Because for many cell types, the membrane state is better described as freestanding, it is also desirable to develop a minimal actin system that is coupled to a freestanding membrane system. Prominent and relatively easy-to-produce freestanding membrane systems are GUVs. We, therefore, transferred the above-mentioned protocol of the coupling of actin filaments to GUVs. The GUVs were formed by electroformation [Angelova and Dimitrov, 1988] of the lipid mixture, which was beforehand dried onto platinum wires and subsequently rehydrated in buffer solution. The lipid composition of the GUVs comprised biotinylated lipids, which couple the actin filaments to the freestanding lipid bilayer, after the subsequent addition of neutravidin and biotinylated actin filaments (Fig. 3A). Between each addition step, the GUVs were washed with buffer solution. We found that actin filaments get anchored to the vesicles forming an actin shell around the GUVs (Fig. 3A). This actin coated GUV system may now be used to study possible changes in the mechanical properties of the GUVs due to the presence of the actin coat. Additionally, possible shape changes triggered by myosin driven contraction may be also a matter for further investigation. Because the GUVs can in principle freely float in solution, one may consider potential movements of some of the GUVs during light microscopic image acquisitions. However, when the GUVs settled down, the actin coat frequently interacted with the glass surface of the microscope slide and thereby provided enough stability for proper imaging. In a previous study by Liu and Fletcher using a GUV system with phase-separating lipids, it was shown that the outside attachment of an actin cytoskeleton mesh affects the phase separation behavior of initially homogeneous GUVs by stabilizing the phase-separated domains [Liu and Fletcher, 2006].

Nevertheless, for some applications, a quasi 2D minimal actin system coupled to a freestanding membrane providing high accessibility to easily remove or add components and supporting high horizontal and vertical stability for proper microscopy may be advantageous. In order to meet these requirements, we developed an in vitro system where membranes are suspended over holes of an electron microscope (EM) grid [Heinemann et al., 2013]. For this purpose, we made use of GUVs comprising the same lipid mixture as used for the other systems with the addition of a small amount of the negatively charged phospholipid DOPG. Because the holey surface of the grid was positively charged due to its prior "silanization," the interaction with the oppositely charged lipids led to a fast rupture of the GUVs after their initial contact with the grid surface (Fig. 3B); see also Heinemann and Schwille [2011]. The remaining membrane comprised a planar lipid bilayer covering holes of the EM grid. With the subsequent addition of neutravidin and biotinylated actin, a quasi 2D MAC was formed where the membrane areas over the grid holes represent freestanding lipid bilayers (Fig. 3B). Also here, the density of the actin layer can be controlled by the concentration of the biotinylated lipids present in the lipid mixture. Because of the high stability of the planar system with respect to horizontal and vertical movements, we were able to perform precise point FCS measurements in order to investigate the lateral diffusion behavior of lipid and protein probes in the presence of coupled actin filaments (Fig. 3C); see also Heinemann et al. [2013]. Former in vivo studies have proposed that the actin mesh influences the lateral diffusion behavior of lipids and proteins within the cell membrane [Sheetz et al., 1980; Kusumi et al., 2005; Andrews et al., 2008; Umemura et al., 2008]. We found, using point FCS measurements, that in our in vitro system, the presence of an actin mesh decreases the lateral mobility of lipid and protein probes (Fig. 3C); see also Heinemann et al. [2013]. The influence on the diffusion behavior strongly depends on the density of the actin meshwork [Heinemann et al., 2013], which can be as well controlled as in the beforehand mentioned in vitro systems.

MAC Formation on Lipid Monolayers

Because of its conceptual simplicity, another intriguing approach to form a planar MAC is the use of lipid monolayers. Here, we make use of a recently developed

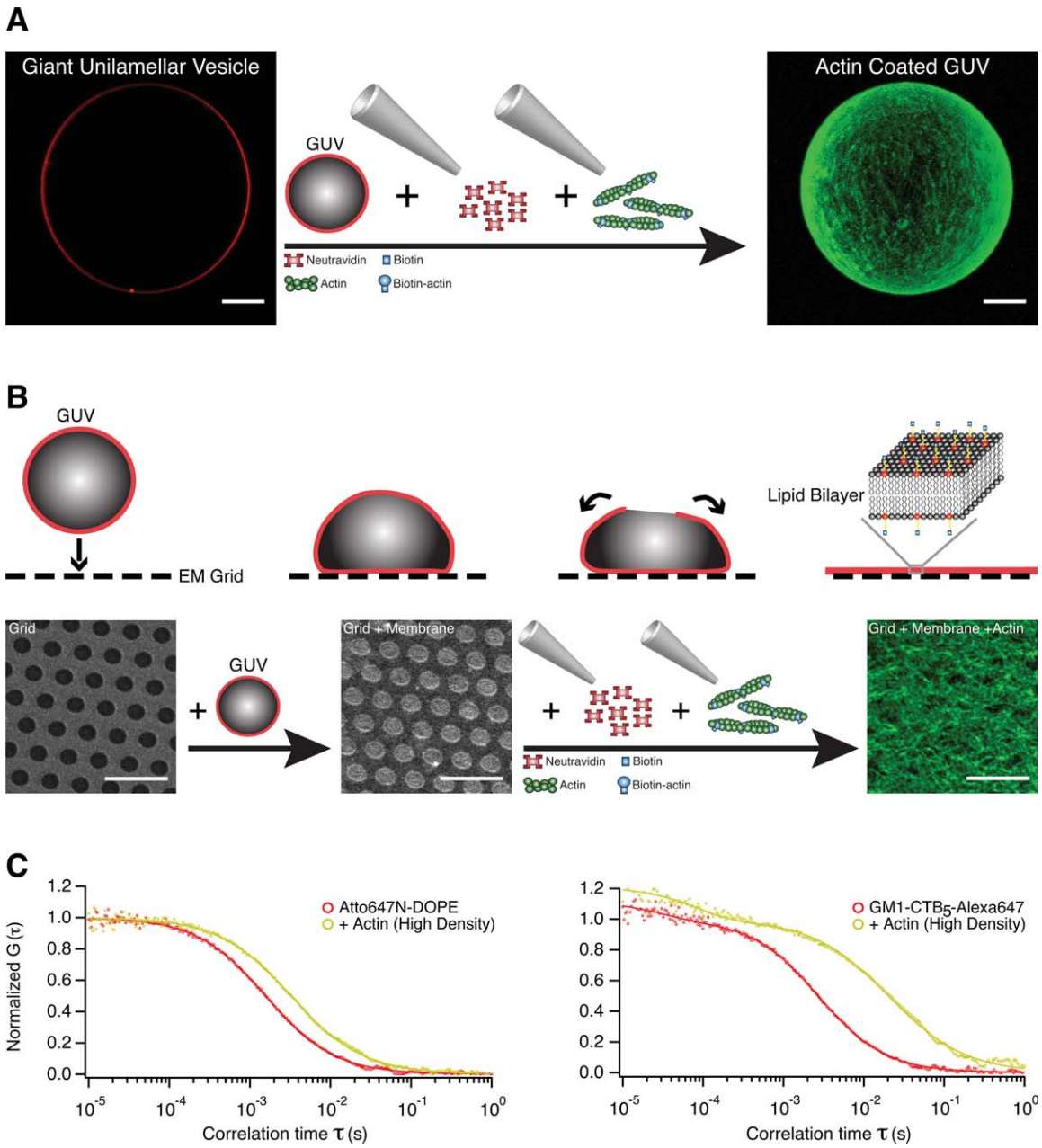

Fig. 3. Actin filaments coupled to freestanding membranes and their effect on lateral lipid and protein diffusion behavior. (**A**) Confocal image (left) at the equatorial plane of an Atto647N-DOPE labeled GUV containing 99 mol % EggPC and 1 mol % DSPE-PEG(2000)-Biotin. Sequential addition of neutravidin and Alexa-488-phalloidin labeled actin filaments to the vesicle resulted in the formation of an actin coated GUV (right image). The right image represents a 3D reconstruction of a confocal image series taken along the vertical axis of the GUV. (**B**) The upper panel shows a schematic drawing describing the sequence of events before and after GUV rupture on an EM grid leading to the formation of suspended freestanding membranes (see also Heinemann and Schwille [2011]). In the lower panel, the left confocal image represents an EM grid. The middle confocal image shows an Atto647N-DOPE labeled membrane suspending the EM grid after landing and rupture of Atto647N-DOPE labeled GUVs. The right confocal image displays Alexa-488-phalloidin labeled actin filaments anchored to the EM grid membrane via neutravidin. (**C**) FCS autocorrelation curves (circles) and corresponding weighted fits (solid lines) of the lipid probe Atto647N-DOPE (left panel) and the protein probe GM1-CholeraToxinB$_5$-Alexa647 (right panel) in the absence (red circles) and presence (yellow circles) of a high density MAC (1 mol % DSPE-PEG(2000)-Biotin). The correlation time increases in the presence of the MAC indicating a decrease in the diffusivity of the probes which was more pronounced in the case of the protein probe. Scale bars, 10 μm.

monolayer assay [Chwastek and Schwille, 2013] with our actin anchoring system. This assay distinguishes itself from the other systems by the fast and easy lipid monolayer preparation, and by the additional degree of freedom of being able to manipulate the lipid density. The lipids, which were first dissolved in chloroform, are added directly to a PTFE chamber filled with an aqueous solution (Fig. 4A). The monolayer forms instantaneously at the air liquid

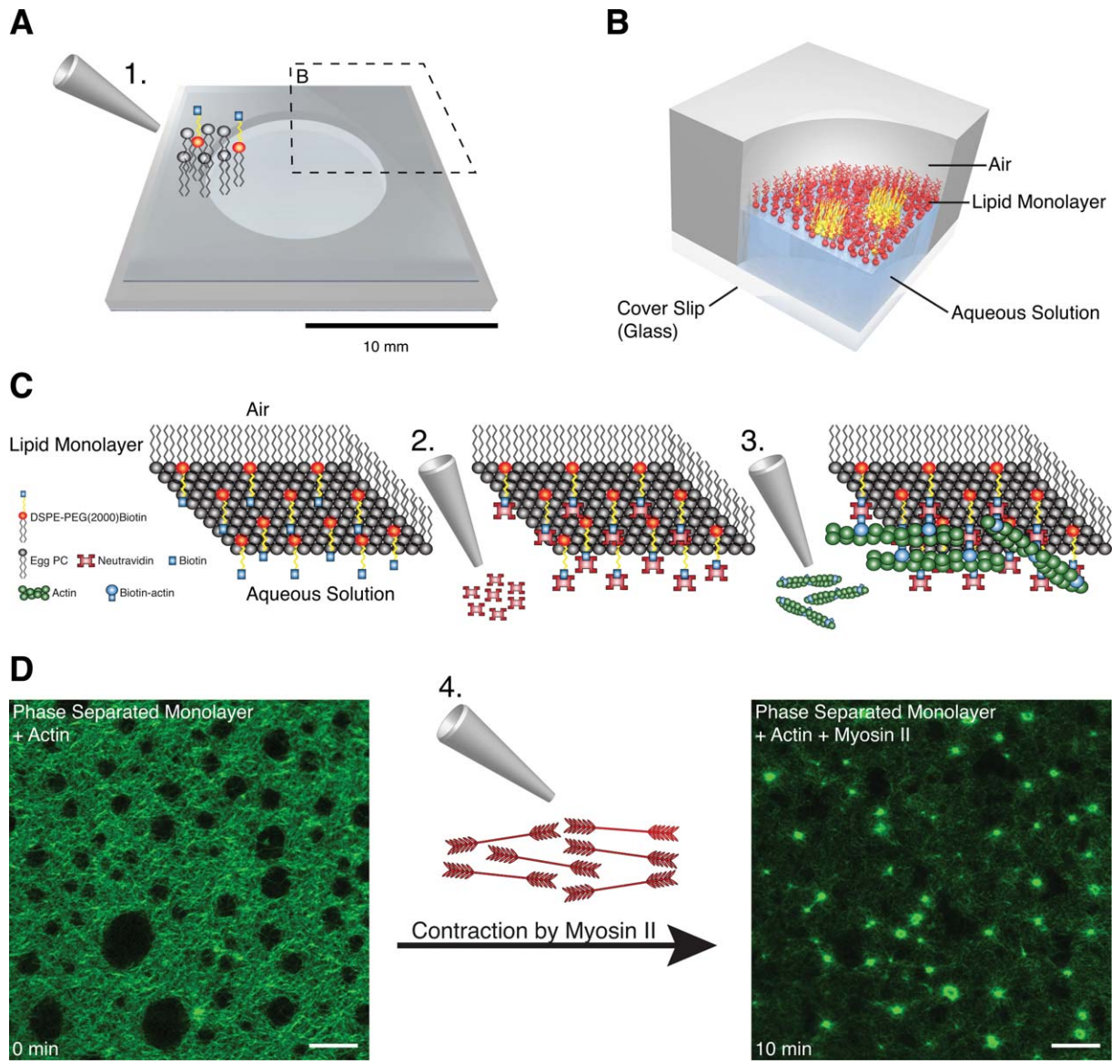

Fig. 4. MAC formation on lipid monolayers and its contraction by myosin motors. (**A**) Schematic drawing of a PTFE chamber filled with aqueous solution. Lipids are deposited on the surface of the solution (step 1) resulting in the formation of the monolayer. Scale bar, 10 mm (referring to the chamber only). (**B**) 3D schematic cross section of the PTFE chamber showing a phase separated lipid monolayer. The lipid expended (disordered) phase is marked in red and the lipid condensed (ordered) domains are depicted in yellow. (**C**) Scheme of a lipid monolayer containing biotinylated lipids where the subsequent addition of neutravidin (step 2) and biotinylated actin filaments (step 3) to the aqueous solution of the system forms an actin mesh coupled to a lipid monolayer. (**D**) Confocal images of Alexa-488-phalloidin labeled actin filaments coupled to a phase separated lipid monolayer before (left image) and after (step 4) the addition of myofilaments (right image). Liquid condensed (ordered) domains are located in the dark round regions without bound actin within the actin meshwork (green). The addition of myofilaments also resulted in the formation of actomyosin clusters (right image) as in the case for lipid bilayers. Scale bars, 10 μm. (Schemes in Figs. A and B adopted and changed from Chwastek and Schwille [2013].

interphase, however, we usually let the system equilibrate for approximately 5 min until the solvent (chloroform) evaporated. The anchor component neutravidin and the actin filaments can now be added to the liquid subphase by dipping the pipette tip through the monolayer (Fig. 4C). With the addition of the necessary components, a 2D actin meshwork that is coupled to the lipid monolayer is formed in a fast and easy manner. By adding and removing buffer solution to the liquid subphase, washing or the addition of further components can be as easily performed as in the other open systems. Besides the ease to form the lipid monolayer, it is of great advantage that membrane properties such as the lipid composition and packing can be adjusted by the further addition of lipids to the system. Thus, complex and difficult lipid mixtures that barely form lipid bilayers on supports or may not form GUVs are accessible through the monolayer assay. We therefore, tested a lipid mixture that formed phase-separated monolayers (Fig.

4B). Because the biotinylated anchor lipids partitioned mainly to the liquid expended (disordered) phase, we found the actin filaments bound to this phase while the liquid condensed (ordered) domains were free of actin filaments (dark areas in Fig. 4D). Subsequent addition of myofilaments to the liquid subphase of the monolayer also resulted in the formation of actomyosin clusters. By varying the membrane properties, such as the lipid packing, one can now investigate the effect of the lipid packing on the formation of the MAC and on the behavior during contraction by the myofilaments.

Discussion

Bottom-up in vitro experiments have the disadvantage that mechanisms derived from them may not necessarily reflect on the physiological complexity of living systems. Nevertheless, the insights gained from these in vitro experiments may describe possible scenarios how a complex cellular process could be driven by a minimal set of components, without the redundancy present in cellular systems. The major advantage of using minimal in vitro systems is the tight control about the systems parameters and the overall quantitative knowledge about the components used in these systems. As a consequence, it is often easier to formulate a physical model based on such well-defined minimal systems, as many parameters can be measured and many assumptions for the theoretical model avoided.

We briefly presented here different approaches how to mimic an actin cell cortex by using supported and freestanding membranes. All techniques have in common that no sophisticated equipment was necessary to build these in vitro systems. In particular, the planar systems were very supportive of light microscopic imaging [total internal reflection fluorescence microscopy (TIRFM), Fig. 1B] and precise single molecule detection methods [e.g., FCS (Fig. 3B) and atomic force microscopy (ATM)]. Owing to the artificial anchoring system using biotinylated lipids and actin filaments, coupled via neutravidin, the actin density in all systems can be varied in a controlled manner by changing the concentration of the biotinylated lipids. Changing the ratio of biotinylated to nonbiotinylated actin monomers can also vary the number of the anchor points within an actin filament. In case of the lipid monolayer system, membrane properties as the lipid packing density can be easily varied by further addition of lipids to the monolayer.

Nevertheless, due to the minimalistic design, our minimal in vitro system has its limitations in mimicking the natural cytoplasmic environment the lipids and proteins are exposed to in living cells, which may also effect the overall behavior of the lipid and protein probes. Hence, for future experiments, it may be interesting to further increase the complexity of the systems by adding more components, for example, to investigate specific functions of proteins or their ability to fine tune the system. To closer mimic, the cytoplasmic in vivo environment measurements could be performed in the presence of cytoplasmic cell extracts and compared with the results obtained from the minimal versions. Therefore, it is very advantageous that in all presented systems components can be added or removed during or after the formation of the MACs. Future studies should also consider the question of how the MAC system would respond to geometrical constraints. To answer this question, components of the MAC systems will have to get encapsulated. Recent work has already proven that is possible to build MACs within liposomes [Pontani et al., 2009; Tsai et al., 2011; Vogel and Schwille, 2012]. Microfluidic techniques [Stachowiak et al., 2008; Abkarian et al., 2011; Matosevic and Paegel, 2011] may help here to control parameters such as liposome size and to increase their number for proper statistical analysis. Since many cell types are not spherical, it will be an interesting challenge to further develop microfluidic techniques to vary the shapes of lipid vesicles in a systematic manner and to test their effect on the MAC and vice versa. With the presentation of our minimal in vitro systems, we aim to trigger the use and further development of such simplified systems mimicking an actin cell cortex, which may reveal possible mechanisms underlying cell shape control through actin-myosin-membrane interactions in the cell cortex.

Material and Methods

Lipids

L-α-phosphatidylcholine (EggPC), 1,2-di-(9Z-octadecenoyl)-*sn*-glycero-3-phosphocholine (DOPC), 1,2-dioleoyl-*sn*-glycero- 3-phospho-(1′-*rac*-glycerol) (DOPG), *N*-(hexadecanoyl)-sphing-4-enine-1-phosphocholine (C16 sphingomyelin), cholesterol, 1,2-distearoyl-*sn*-glycero-3-phosphoethanolamine-*N*-[biotinyl-(polyethyleneglycol)-2000] (DSPE-PEG(2000)-Biotin) and Ganglioside GM1 (GM1) were purchased from Avanti (Alabaster, AL). 1,2-dioleoyl-*sn*-glycero-3 phosphoethanolamine headgroup labeled with Atto647N (Atto647N-DOPE) was obtained from Atto-Tec (Siegen, Germany).

Actin Preparation and Labeling

Rabbit skeletal muscle actin monomers (Molecular Probes) and biotinylated rabbit actin monomers [tebu-bio (Cytoskeleton, Offenbach, Germany)] were mixed in a 4:1 ratio, respectively. Polymerization of the mixture (39.6 μM) was induced in F-buffer containing 50 mM KCl, 2 mM $MgCl_2$, 1 mM DTT, 1 mM ATP, 10 mM Tris-HCl buffer (pH 7.5). The biotinylated actin filaments were labeled with Alexa-Fluor 488 Phalloidin (Molecular Probes) following the protocol of the manufacturer obtaining 2 μM (refers to monomers) of Alexa-488-Phalloidin-stabilized biotinylated actin filaments. Alternatively, to get dynamic actin filaments, unlabeled, biotinylated and Alexa-488-Actin monomers (molecular probes) were mixed in a 8:2:1

ratio, respectively, obtaining a concentration of 4 μM (refers to monomers).

Myosin Preparation

Myosin was purified from rabbit skeletal muscle tissue as previously described [Smith et al., 2007]. The activity of the purified myosin motors was tested using a motility assay where single myosin motors bound to a nitrocellulose coated glass surface of a perfusion chamber (tebu-bio, Cytoskeleton) propel actin filaments. Actin filaments were moved by the myosin motors indicating their proper function. The assembly of myosin motors to form myofilaments was induced in reaction buffer containing 50 mM KCl, 2 mM $MgCl_2$, 1 mM DTT, and 10 mM Tris-HCl buffer (pH 7.5), and depending on the experiments various amounts of regenerated ATP (see below) and an oxygen scavenger system (see below).

MAC Contraction by Myofilaments

Myofilaments (0.3 μM) dissolved in 200 μl reaction buffer were added to the MAC systems and imaged by total internal reflection fluorescence (TIRF) or confocal microscopy. The reaction buffer contained 1 μM ATP in the case when an ATP regenerating system consisting of 20- mM Creatine phosphate (Sigma) and 0.1 mg ml^{-1} Creatine phospho kinase (Sigma) to keep the ATP concentration constant was used and an oxygen scavenger system [glucose oxidase (165 U ml^{-1}), catalase (2170 U ml^{-1}), β-D-glucose (0.4% w/v), and Trolox (2 mM), all from Sigma] to reduce photobleaching of the Alexa dyes. Actin contraction occurred immediately after addition of the myofilaments in all described MAC systems. The ATP concentration was not regenerated in the results shown in Fig. 2B and the starting ATP concentration was 4 mM (Fig. 2B, left image). After depletion of the ATP concentration and the concurrent contraction of the MAC (Fig. 2B, middle image), the ATP concentration was readjusted to approximately 4 mM (Fig. 2B, right image).

MAC Preparation on Supported Lipid Bilayers

For MAC preparation on a glass support, a chamber consisting of a cut 1.5 ml Eppendorf tube glued to an air plasma-cleaned glass cover slip (22 × 22 mm, #1.5, Menzel Gläser, Thermo Fisher, Braunschweig, Germany) was built (see also Vogel et al. [2013]). For lipid bilayer formation on the glass support, molar ratios of the lipids EggPC (99.99, 99.9, and 99 mol %) and DSPE-PEG(2000)-Biotin (0.01, 0.1, and 1 mol %), respectively, were dissolved in chloroform (total 10 mg/ml of lipids), dried under nitrogen flux for 30 min and subsequently put into vacuum for 30 min. Lipids were then rehydrated in reaction buffer and resuspended by vigorous vortexing. To obtain SUVs (small unilamellar vesicles), the suspension was exposed to sonication in an ultrasonic water bath at room temperature. 10 μl of the suspension were mixed with 90 μl buffer and placed onto the glass coverslip of the chamber. $CaCl_2$ to a final concentration of 0.1 mM was added to induce fusion of the SUVs and the formation of a lipid bilayer on the glass surface. In order to remove unfused vesicles, the sample was washed several times with a total volume of approximately 2 ml. After washing, 200 μl of neutravidin (molecular probes) solution (0.0025 μg/μl) was added to the sample and incubated at room temperature for 10 min. The sample was washed several times with >2 ml buffer to remove unbound neutravidin. After that, 10–50 μl of 2 μM (refers to monomers) Alexa-488-phalloidin labeled (stabilized) or Alexa-488 labeled (dynamic) biotinylated actin filaments were added to the lipid bilayer and incubated for 1 h. The sample was carefully washed with approximately 1–2 ml buffer to remove unbound actin filaments (in the case of phalloidin-stabilized actin filaments).

Giant Unilamellar Vesicle (GUV) Preparation

GUVs were prepared by the electroformation method [Angelova and Dimitrov, 1988]. 5 μl of 1 mg/ml in chloroform dissolved lipids [EggPC (mol 98.9%), DSPE-PEG(2000)-Biotin (1 mol %), Atto647N-DOPE (0.1 mol %)] were deposited on two Pt wires in a polytetrafluorethylen (PTFE) chamber. After evaporation of the solvent, the chamber was filled with 300 μl sucrose (300 mM) solution and exposed to 2 V AC current at 10 Hz for 1 h and subsequently at 2 Hz for 30 min. 200 μl (0.0025 μg/μl) neutravidin was added to the GUV containing sucrose solution and incubated for 5 min. Then 20 μl of the GUV suspension was added to a cut 2.5 ml Eppendorf tube glued onto a glass microscope slide (#1.5, Menzel Gläser, Thermo Fisher, Braunschweig, Germany) containing 2 ml of reaction buffer and Alexa-488-phalloidin labeled actin filaments. Due to the higher density of the sucrose within the GUVs, they will settle down and actin filaments will anchor to the neutravidin to form an actin filament shell around the GUV (see main text Fig. 3A).

Suspended Freestanding Membrane Preparation

An EM grid (2.5 μm hole diameter, Ted Pella, Redding, CA, USA) consisting of a holey Si_3N_4 support film was silanized with the triaminosilane (3-trimethoxysilylpropyl) diethylenetriamine (DETA, Sigma-Aldrich, St. Louis, MO, USA). The silanized grid was mounted on a round glass slide (d = 24 mm, #1.5, Menzel Gläser, Thermo Fisher Scientific, Braunschweig, Germany) by using small stripes of double-sided tape. A closed chamber was assembled using a cover slip holder (CoverSlipHolder, JPK, Berlin, Germany). The chamber was filled with 400 μl buffer. GUVs were prepared by electroformation in 300 mM sucrose as described beforehand. Cholera toxin subunit B-Alexa 647 (CtxB-Alexa647) was obtained from Molecular Probes. For fluorescence

correlation spectroscopy (FCS) experiments with the labeled lipid Atto647N-DOPE GUVs were prepared with a lipid mixture consisting of EggPC (97.495 mol %), DSPE-PEG(2000)-Biotin (2 mol %), DOPG (0.5 mol %), and Atto647N-DOPE (0.005 mol %). For experiments with the GM1 binding protein CtxB, GUVs were prepared with a lipid mixture consisting of EggPC (97.47 mol %), DSPE-PEG(2000)-Biotin (2% mol), DOPG (0.5 mol %), and GM1 (0.03 mol %). After GUV formation, they were added to the silanized grid. GUVs settled down to the grid due to the higher density of the sucrose solution in the GUVs. After ~5–15 min, most of the GUVs ruptured and freestanding membranes were formed on the surface. Residual sucrose was removed by repetitive washing with buffer solution. In case of experiments involving CtxB, the membrane labeling was performed by adding 20 μL of 5 μg/ml CtxB-Alexa647. The system was incubated for 10 min and washed several times with buffer solution to remove unbound CtxB-Alexa647. For further details, see also Heinemann et al. [2013].

Lipid Monolayer Preparation

The lipids DOPC, C16 sphingomyelin and cholesterol were mixed in a 3:3:1 ratio dissolved in chloroform with a total lipid concentration of 0.1 mg/ml. To form a chamber (see Figs. 4A and 4B), chamber spacers were cut from a 1 mm thick sheet of PTFE by a laser cutter (Trotec Laser, Ypsilanti, MI) (for details, see also Chwastek and Schwille [2013]). Glass cover slips (Gerhard Menzel GmbH, Braunschweig, Germany) were fixed to the spacer by UV-curable glue 63 Norland Products (Cranbury, NJ). The chambers were washed alternately with ethanol and water, dried and air plasma-cleaned for 10 min in order to make the glass hydrophilic. Lipid monolayers were formed by drop-wise addition of the lipid composition (dissolved in chloroform) on the water-air interface. 4.1 μl of the lipid mixture was deposited drop-wise on the surface of the buffer solution. Samples were imaged using a confocal laser scanning microscope (see above) equipped with LD C-Apochromat (40×, 1.1 NA) Zeiss objective with a working distance of 0.62 mm. After the formation of a phase separated lipid monolayer was confirmed with confocal microscopy 100 μl of neutravidin solution (0.01 μg/μl) was added to the sample and was incubated for 5 min. Note that in general protein solutions or other components and solutions are applied to the liquid subphase by dipping the pipette tip through the monolayer. Subsequently, the monolayer was washed with reaction buffer several times (each time 100 μl) to remove unbound neutravidin and 100 μl of Alexa-488-phalloidin labeled actin filaments (2 μM) was added to the subphase. Since binding of actin filaments to the interface was assumed to occur relatively slowly, the sample was incubated at least 30 min and then washed several times with 100 μl of reaction buffer. When the binding of the actin filaments was confirmed by confocal imaging 100 μl of myofilaments (0.3 μM) containing 1 μM ATP (enzymatically regenerated see above) was added to the subphase. The lipid monolayer MAC system started to contract immediately after addition of the myofilaments resulting in the formation of actomyosin clusters.

TIRF and Confocal Microscopy

TIRF microscopy was carried out on a custom-made setup built around an Axiovert 200 microscope (Zeiss). An α Plan-Apochromat 100×/NA 1.46 oil immersion objective and a 488-nm laser line was used for excitation of the labeled probes. The exposure times were 100 ms, and the time intervals between each recorded frame ranged from 200 to 400 ms for different experiments.

For confocal imaging, the samples were imaged using a confocal laser scanning microscope (LSM 510, ConfoCor2, Zeiss, Jena, Germany) equipped with a 40× LD (long distance C-Apochromat, 1.1 NA, Carl Zeiss) objective with a working distance of 0.62 mm or with a 40× water immersion objective (C-Apochromat, NA 1.2, Carl Zeiss). The phalloidin-Alexa488 labeled actin was excited with the 488-nm line of an Ar-ion laser; the membrane (labeled either by Atto647N-DOPE or CtxB-Alexa647) was excited with the 633-nm line of a He-Ne laser. HFT 488/633 and NFT 635 dichroic mirrors were used to split the excitation and fluorescence emission. A λ/4 plate was used to achieve excitation by circular polarized light. For concurrent imaging of the membrane and actin, a 505–560-nm band bass (actin channel) and a 655-nm long pass filter (membrane channel) were used in front of the detection channels.

Single Point Fluorescence Correlation Spectroscopy

Point FCS for the experiments to correlate the presence of a high actin density mesh with the lipid and protein probe mobility was performed on a LSM 510 Meta confocal microscope (Carl Zeiss, Jena, Germany) using a 40× water immersion objective (C-Apochromat, NA 1.2, Carl Zeiss). The Alexa-488-phalloidin labeled actin filaments were excited with the 488-nm line of an Ar-ion laser; the membrane (labeled either by Atto647N-DOPE or CtxB-Alexa647) was excited with the 633-nm line of a He-Ne laser. FCS was performed using a home-build detection unit at the optical fiber output channel of the LSM 510. A band pass filter (HQ 700/75, AHF Analysentechnik, Tübingen, Germany) was used to reject scattered or reflected laser light. The fluorescence was detected by avalanche photodiodes (PerkinElmer, San Jose, CA) and the fluorescence autocorrelation $G(t)$ obtained by using a hardware correlator (Flex 02-01D, correlator.com, Bridgewater, NJ). A laser power of 0.95 μW was used for imaging the Alexa-488-phalloidin labeled actin filaments to avoid photobleaching. For further details, see also the Supporting Information in Heinemann et al. [2013].

Data Analysis

Data analysis was performed with Image J (Rasband, W.S., National Institutes of Health, http://imagej.nih.gpv/ij) and custom written scripts in Igor Pro 6.0 (WaveMetrics, Lake Oswego, OR, USA) and MatLab.

Acknowledgments

The authors are grateful for the financial support provided by the Daimler und Benz foundation to S.K.V. and F.H. (Grant 32-09/11), and the Gottfried Wilhelm Leibniz- Program of the DFG to S.K.V. and G.C. (SCHW716/8-1).

References

Abkarian M, Loiseau E, Massiera G. 2011. Continuous droplet interface crossing encapsulation (cDICE) for high throughput monodisperse vesicle design. Soft Matter 7(10):4610–4614.

Andrews NL, Lidke KA, Pfeiffer JR, Burns AR, Wilson BS, Oliver JM, Lidke DS. 2008. Actin restricts FcepsilonRI diffusion and facilitates antigen-induced receptor immobilization. Nat Cell Biol 10(8): 955–963.

Angelova M, Dimitrov DS. 1988. A mechanism of liposome electroformation. Prog Colloid Polym Sci 76:59–67.

Backouche F, Haviv L, Groswasser D, Bernheim-Groswasser A. 2006. Active gels: Dynamics of patterning and self-organization. Phys Biol 3(4):264–273.

Balasubramanian MK, Srinivasan R, Huang Y, Ng KH. 2012. Comparing contractile apparatus-driven cytokinesis mechanisms across kingdoms. Cytoskeleton (Hoboken) 69(11):942–56.

Barfoot RJ, Sheikh KH, Johnson BR, Colyer J, Miles RE, Jeuken LJ, Bushby RJ, Evans SD. 2008. Minimal F-actin cytoskeletal system for planar supported phospholipid bilayers. Langmuir 24(13): 6827–6836.

Blanchoin L, Amann KJ, Higgs HN, Marchand JB, Kaiser DA, Pollard TD. 2000. Direct observation of dendritic actin filament networks nucleated by Arp2/3 complex and WASP/Scar proteins. Nature 404(6781):1007–1011.

Bosk S, Braunger JA, Gerke V, Steinem C. 2011. Activation of F-actin binding capacity of ezrin: Synergism of PIP interaction and phosphorylation. Biophys J 100(7):1708–1717.

Chwastek G, Schwille P. 2013. A monolayer assay tailored to investigate lipid-protein systems. ChemPhysChem 14(9):1877–1881.

Cramer LP, Mitchison TJ. 1995. Myosin is involved in postmitotic cell spreading. J Cell Biol 131(1):179–189.

Deme B, Hess D, Tristl M, Lee LT, Sackmann E. 2000. Binding of actin filaments to charged lipid monolayers: Film balance experiments combined with neutron reflectivity. Eur Phys J E 2(2):125–136.

Glotzer M. 2005. The molecular requirements for cytokinesis. Science 307(5716):1735–1739.

Gordon D, Bernheim-Groswasser A, Keasar C, Farago O. 2012. Hierarchical self-organization of cytoskeletal active networks. Phys Biol 9(2):026005.

Guha M, Zhou M, Wang YL. 2005. Cortical actin turnover during cytokinesis requires myosin II. Curr Biol 15(8):732–736.

Hackl W, Barmann M, Sackmann E. 1998. Shape changes of self-assembled actin bilayer composite membranes. Phys Rev Lett 80(8): 1786–1789.

Heinemann F, Schwille P. 2011. Preparation of micrometer sized free-standing membranes. ChemPhysChem 12(14):2568–2571.

Heinemann F, Vogel SK, Schwille P. 2013. Lateral membrane diffusion modulated by a minimal actin cortex. Biophys J 104(7):1465–1475.

Heisenberg CP, Bellaiche Y. 2013. Forces in tissue morphogenesis and patterning. Cell 153(5):948–962.

Ikai A, Afrin R. 2003. Toward mechanical manipulations of cell membranes and membrane proteins using an atomic force microscope: An invited review. Cell Biochem Biophys 39(3):257–277.

Imamura H, Nhat KP, Togawa H, Saito K, Iino R, Kato-Yamada Y, Nagai T, Noji H. 2009. Visualization of ATP levels inside single living cells with fluorescence resonance energy transfer-based genetically encoded indicators. Proc Natl Acad Sci U S A 106(37): 15651–15656.

Janke M, Herrig A, Austermann J, Gerke V, Steinem C, Janshoff A. 2008. Actin binding of ezrin is activated by specific recognition of PIP2-functionalized lipid bilayers. Biochemistry 47(12):3762–3769.

Johnson BR, Bushby RJ, Colyer J, Evans SD. 2006. Self-assembly of actin scaffolds at ponticulin-containing supported phospholipid bilayers. Biophys J 90(3):L21–L23.

Kohler S, Schaller V, Bausch AR. 2011. Structure formation in active networks. Nat Mater 10(6):462–468.

Kusumi A, Nakada C, Ritchie K, Murase K, Suzuki K, Murakoshi H, Kasai RS, Kondo J, Fujiwara T. 2005. Paradigm shift of the plasma membrane concept from the two-dimensional continuum fluid to the partitioned fluid: High-speed single-molecule tracking of membrane molecules. Annu Rev Biophys Biomol Struct 34:351–378.

Lee K, Gallop JL, Rambani K, Kirschner MW. 2010. Self-assembly of filopodia-like structures on supported lipid bilayers. Science 329(5997):1341–1345.

Limozin L, Barmann M, Sackmann E. 2003. On the organization of self-assembled actin networks in giant vesicles. Eur Phys J E Soft Matter 10(4):319–330.

Limozin L, Roth A, Sackmann E. 2005. Microviscoelastic moduli of biomimetic cell envelopes. Phys Rev Lett 95(17):178101.

Liu AP, Fletcher DA. 2006. Actin polymerization serves as a membrane domain switch in model lipid bilayers. Biophys J 91(11): 4064–4070.

Loisel TP, Boujemaa R, Pantaloni D, Carlier MF. 1999. Reconstitution of actin-based motility of Listeria and Shigella using pure proteins. Nature 401(6753):613–616.

Matosevic S, Paegel BM. 2011. Stepwise synthesis of giant unilamellar vesicles on a microfluidic assembly line. J Am Chem Soc 133(9):2798–2800.

Merkle D, Kahya N, Schwille P. 2008. Reconstitution and anchoring of cytoskeleton inside giant unilamellar vesicles. Chembiochem 9(16):2673–2681.

Mitchison T, Kirschner M. 1984. Dynamic instability of microtubule growth. Nature 312(5991):237–242.

Murrell MP, Gardel ML. 2012. F-actin buckling coordinates contractility and severing in a biomimetic actomyosin cortex. Proc Natl Acad Sci U S A 109(51):20820–20825.

Murthy K, Wadsworth P. 2005. Myosin-II-dependent localization and dynamics of F-actin during cytokinesis. Curr Biol 15(8):724–731.

Pontani LL, van der Gucht J, Salbreux G, Heuvingh J, Joanny JF, Sykes C. 2009. Reconstitution of an actin cortex inside a liposome. Biophys J 96(1):192–198.

Sheetz MP, Schindler M, Koppel DE. 1980. Lateral mobility of integral membrane proteins is increased in spherocytic erythrocytes. Nature 285:510–512.

Smith D, Ziebert F, Humphrey D, Duggan C, Steinbeck M, Zimmermann W, Kas J. 2007. Molecular motor-induced instabilities and cross linkers determine biopolymer organization. Biophys J 93(12):4445–4452.

Soares e Silva M, Depken M, Stuhrmann B, Korsten M, MacKintosh FC, Koenderink GH. 2011. Active multistage coarsening of actin networks driven by myosin motors. Proc Natl Acad Sci U S A 108(23):9408–9413.

Spudich JA, Kron SJ, Sheetz MP. 1985. Movement of myosin-coated beads on oriented filaments reconstituted from purified actin. Nature 315(6020):584–586.

Stachowiak JC, Richmond DL, Li TH, Liu AP, Parekh SH, Fletcher DA. 2008. Unilamellar vesicle formation and encapsulation by microfluidic jetting. Proc Natl Acad Sci U S A 105(12):4697–4702.

Tamm LK, McConnell HM. 1985. Supported phospholipid bilayers. Biophys J 47(1):105–113.

Tanaka M, Sackmann E. 2005. Polymer-supported membranes as models of the cell surface. Nature 437(7059):656–663.

Tsai FC, Stuhrmann B, Koenderink GH. 2011. Encapsulation of active cytoskeletal protein networks in cell-sized liposomes. Langmuir 27(16):10061–10071.

Umemura YM, Vrljic M, Nishimura SY, Fujiwara TK, Suzuki KGN, Kusumi A. 2008. Both MHC class II and its GPI-anchored form undergo hop diffusion as observed by single-molecule tracking. Biophys J 95(1):435–450.

Vale RD, Reese TS, Sheetz MP. 1985. Identification of a novel force-generating protein, kinesin, involved in microtubule-based motility. Cell 42(1):39–50.

Vogel SK, Schwille P. 2012. Minimal systems to study membrane-cytoskeleton interactions. Curr Opin Biotechnol 23:758–765.

Vogel SK, Petrasek Z, Heinemann F, Schwille P. 2013. Myosin motors fragment and compact membrane-bound actin filaments. ELife 2:e00116.

Wessells NK, Spooner BS, Ash JF, Bradley MO, Luduena MA, Taylor EL, Wrenn JT, Yamaa K. 1971. Microfilaments in cellular and developmental processes. Science 171(3967):135–143.

Wu JQ, Sirotkin V, Kovar DR, Lord M, Beltzner CC, Kuhn JR, Pollard TD. 2006. Assembly of the cytokinetic contractile ring from a broad band of nodes in fission yeast. J Cell Biol 174(3):391–402.